Available online at www.sciencedirect.com
SCIENCE DIRECT®
Solar Energy Materials & Solar Cells
ELSEVIER
Solar Energy Materials & Solar Cells 81 (2004) 73–86
www.elsevier.com/locate/solmat

Computer-aided band gap engineering and experimental verification of amorphous silicon–germanium solar cells

Raul Jimenez Zambrano[a], Francisco A. Rubinelli[b], Wim M. Arnoldbik[c], Jatindra K. Rath[a,*], Ruud E.I. Schropp[a]

[a] *Debye Institute, Utrecht University, SID-Physics of Devices, P.O. Box 80000, NL-3508 TA Utrecht, The Netherlands*
[b] *INTEC, Universidad Nacional del Litoral, Guemes 3450, 3000, Santa Fe, Argentina*
[c] *Debye Institute, Utrecht University, SID-Functional Materials, P. O. Box 80000, NL-3508 TA Utrecht, The Netherlands*

Received 11 July 2003; accepted 4 August 2003

Abstract

A new band gap profile (exponential profile) for the active layer of the a-SiGe:H single junction cell has been designed and experimentally demonstrated. By computer simulations we show how bending the grading of the band gap in the i-layer contributes to the enhancement of the carrier collection, improving the fill factor and efficiency. The differences observed between experiments and simulations are studied using Rutherford Backscattering Spectrometry (RBS). The results highlight weak points during the deposition process, whose control enables us to bring together experimental and computational results.

Keywords: Band gap design; a-SiGe:H; Solar cells; Ge diffusion

1. Introduction

The optical characteristics of hydrogenated amorphous silicon–germanium alloys (a-SiGe:H) allow them to be widely used as low band gap material for multijunction

*Corresponding author. Ornstein Laboratory, Department of Atomic and Interface Physics, Debye Institute, Princeton Plein 1, P.O. Box 80000, Utrecht 3508 TA, Netherlands. Tel.: +31-30-253-2961; fax: +31-30-254-3165.
E-mail address: j.k.rath@phys.uu.nl (J.K. Rath).

0927-0248/$ - see front matter
doi:10.1016/j.solmat.2003.08.017

solar cells. Alloying of a-Si:H with Ge reduces the band gap to tune the optical band gap, and increases the absorption coefficient at long wavelengths. However, the electronic properties deteriorate with increasing Ge content due to the increased density of midgap states, which influences the recombination rate and the field profile within the device. To overcome the limitations caused by the electronic properties of a-SiGe:H, the introduction of a band gap profile in the active layer of a-SiGe:H single junction cells has been previously proposed and implemented [1]. The band gap profile of the intrinsic layer redistributes the space charges that determine the screening of the electric field within the device. Thus, the profile determines the spatial electric field within the device and the collection of the photo generated carriers. Moreover, such structures help to alter the recombination losses and to improve the carrier collection in the i-layer.

In this paper we propose a new band gap grading, namely exponential band gap grading (E-shape) profile, which has a distinct advantage with respect to the generation and collection of photo-generated carriers and leads to low recombination losses.

We present our results by coupling computer simulations and experiments in which this is implemented in a p–i–n single junction solar cell. The advantages of this new profile are compared to the two profiles most commonly used at present, the U-shape band gap grading [2] and the V-shape band gap grading [1,3] profiles.

Though the beneficial aspect of the exponential profile was observed in the experiments, we observed a deviation between the simulation predictions and the experimental results in the details of the cell behavior. This could be related to a lack of immediate relation between the change in the flow of germane and the incorporation of Ge in the material, occurring principally when the changes in flow are not uniform, as is the case in any non-linear profile. In the absence of proper composition depth profiling techniques, this would lead to a lack of control of the band gap profiling, generating profiles that deviate from the intended design. We employed Rutherford Back Scattering (RBS) to aid in obtaining the intended band gap profiles.

2. Experiments

The p–i–n amorphous silicon–germanium alloy solar cells studied in this research were grown in an ultrahigh vacuum multi-chamber system (PASTA) by Plasma Enhanced Chemical Vapor Deposition (PECVD). The substrates were textured SnO_2 coated on glass (Asahi U-type). There was no TCO at the back contact, between the n-layer and the metal (Ag) for optical enhancement. Deposition of the i-layer was done at a substrate temperature of 200°C, at a pressure of 1.65 Torr and an RF power density of $42\,mW\,cm^{-2}$. The structure of the devices included a graded a-SiGe:H layer separated from the doped layers at both sides by buffers made of a-Si:H. By varying the germane flow during deposition, the graded a-SiGe:H intrinsic layers are fabricated as staircase profiles of four steps between the buffer layers and the lowest band gap (1.55 eV) layer. The band gap $E_G = E_{3.5}$ of the films

was obtained from the reflection and transmission optical measurements, identifying the band gap to the photon energy at which the absorption coefficient is $10^{3.5}\,cm^{-1}$. Current–voltage (I/V) measurements of single a-SiGe:H cells were carried out in the dark, under AM 1.5 light and with filtered light. As a filter, a 100 nm a-Si:H layer on a glass substrate was used to simulate the light that reaches the bottom cell in a tandem structure.

The RBS measurements were done on a-SiGe:H samples deposited on a c-Si wafer. These samples have the same staircase profiles as the single junction cell but without the doped and the buffer layers. The composition profile of the samples was probed with 1.5 MeV He^+ ions.

3. Results and discussion

3.1. Modeling

Our simulations were performed with the computer code D-AMPS that stands for AMPS' core (analysis of microelectronic and photonic devices developed at The Pennsylvania State University, USA [4]) plus some new developments. These new developments refer to the inclusion in AMPS of amphoteric states [5], the defect pool model [6,7] and scattering at rough surfaces [8].

A typical a-SiGe:H band gap structure studied in this research is showed in Fig. 1. It shows the band diagram of the p–i–n a-SiGe:H at short circuit conditions calculated by D-AMPS under AM 1.5 illumination. The doped p and n layers, separated from the intrinsic layer by a front and a back buffer are represented. The intrinsic layer consists of a 4-step staircase front grading between the p-layer and the uniform lowest band gap layer, and a 4-step staircase back grading between this last layer and the n-layer.

For fitting purposes some opto-electronic parameters of the various materials that make up the solar cell were measured. The electrical parameters that cannot be

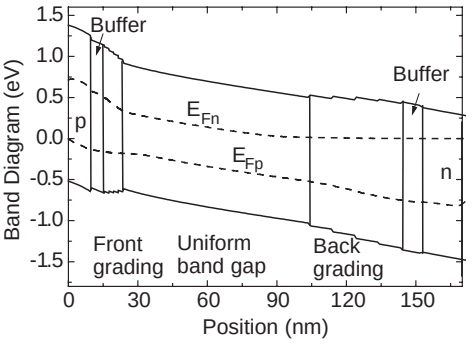

Fig. 1. Computer-generated band diagram of the a-SiGe:H p–i–n solar cell at short circuit conditions. The quasi-Fermi levels for electrons (E_{Fn}) and holes (E_{Fp}) are shown by dotted lines.

directly measured were adopted as equal to standard values found in the literature or those from the best fits to our experimental curves.

The energy distribution of defect states in the band gap as a function of the alloy contribution is controversial [9,10]. Calculations by Stiebig [11], realized from CPM and PDS measurements on a-SiGe:H with a wide range of Ge concentrations, suggest that, while by electron spin resonance (ESR) measurements Si-related dangling bonds can be distinguished from Ge-related dangling bonds, the comparison of the calculations between CPM and PDS spectra does not reveal a significant difference between the capture cross sections or energy position for Si- and Ge-related dangling bonds. The defect distribution adopted in this study considers only one type of defect with a single capture cross section.

Sensitivity studies were performed for several parameters to determine their influences over the solar cell characteristics (especially the band gap, electron and hole mobility, charged and neutral cross section, valence band tail slope, offset of the band gap and total density of states). A relation between some of the parameters used for the simulation has been consistently observed. As an example some of these relations are listed. The band gap of the a-Si:H is lowered continuously by alloying with germanium [12]. The total density of states increases exponentially with decreasing the band gap [13]. The Urbach tail, which reflects the valence band tail, increases linearly with decreasing the band gap [14].

To probe the consistence of the results present, simulations have been carried out where the set of parameters used did not closely fit the experimental results. On the other hand the variations of the set of parameters selected were done keeping, in between others, the established relations mentioned above. The trends present in this study are observed independent of the set of parameters. This permits to consider the tendencies as a real behavior, independent of the set of parameters chosen, even when these parameters are selected to fit the experimental results.

Modeling the density of dangling bonds in each device layer can be accomplished by using either the standard uniform density profile or the defect pool model. Some work has been done [15] to study the influence of these models on the p/i interface, since with the uniform model an extra defect layer has to be included to reproduce experimental data.

In a previous investigation [16] we studied the single junction a-SiGe:H p–i–n solar cell in the annealed state using D-AMPS. To understand the influence of these models in the complete behavior of the solar cell, we modeled the density of dangling bond states using these two different electrical approaches: (a) uniform density model of gap states in each layer of the device (UDM) and (b) the defect pool model as proposed by Powell and Deane [6,7] (DPM). We were able to fit the dark and the illuminated current voltage characteristics and the spectral response curve under short circuit conditions using either uniform density of states in each layer or the defect pool model. When we modeled each layer of a-SiGe:H p–i–n solar cells with a uniform density of states we were not able to explain the advantages of introducing a V-shaped band gap profile in the a-SiGe:H intrinsic layer. On the other hand implementing the defect pool model in our computer code we were able to predict an optimum thickness for the front buffer layer and for the front band gap graded

layers. We concluded that to properly design the band gap profile in a-SiGe:H solar cells in particular and to appropriately model a-Si:H based solar cells in general it is necessary to include the defect pool model in any computer simulations.

To optimize the performance of the single junction p–i–n a-SiGe:H solar cell, we therefore further make use of D-AMPS with the defect pool model to describe the density of dangling bonds states. We designed a new band gap profile that is described in the following section.

3.2. *Influence of the band gap profile*

The profiling of the band gap of the intrinsic layer modifies simultaneously the distribution of the trapped charge and the electric field profile, which strongly influences the recombination rate. An appropriate band gap profile leads to a reduction in the recombination losses and to an improvement in the carrier collection within the i-layer.

We begin by studying the losses that are present in the U- and V-shape band gap profile. We will compare both profiles with the exponential profile (E-profile), which is designed for application in an a-SiGe:H bottom cell of a tandem structure.

The U-shape band gap profile used in the intrinsic a-SiGe:H layer of our solar cells, presents a short front grading ($\sim$10 nm), a long uniform low band gap layer ($\sim$70 nm and 1.5 eV) and a long back grading ($\sim$40 nm). Fig. 2 shows the schematic U-shape i-layer band gap profile, excluding the buffer layers. The other two profiles in this figure are the V- and E-shape profile. These two profiles are simulated starting from the U-shape profile by modifying only the thickness of the layers that form the i-layer. The same is done for the deposition of the solar cells where the only parameter modified is the deposition time of the layers.

The recombination losses in these structures have been studied in detail by simulating the cell with the computer code D-AMPS. Looking at the recombination profile at different forward bias voltages and for filtered light for the U-shape band gap profile (Fig. 3) it is observed how the main recombination region shifts from the

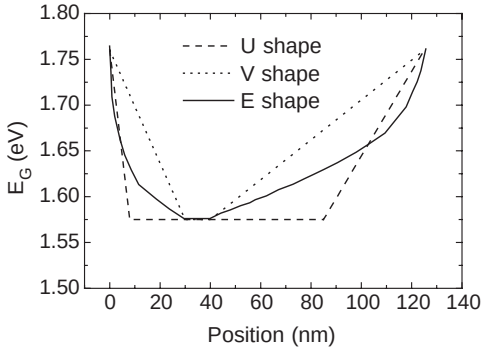

Fig. 2. Schematic i-layer band gap profiling of the 'U-shape', 'V-shape' and 'E-shape' structures, without buffer layer.

rear part of the bulk, for 0 V bias, to the bulk at forward biases and to mostly the front of the bulk, near the p/i junction, for 0.6 V (a value close to the open circuit voltage, V_{oc}).

The recombination current is directly responsible for the fill factor (FF) of the solar cell. It also has a significant influence on the V_{oc}. If the dark $I-V$ characteristics of an a-Si:H alloy solar cell are shifted by the short circuit current (J_{sc}) value under illumination (assuming that the superposition principle is valid), we end up with a V_{oc} that is significantly higher than the real V_{oc}. This is due to the rather large density of defects that is present in a-Si:H alloys, producing large recombination currents at forward voltages. Fig. 4 shows the difference between the generation rate and the recombination rate for different forward voltages under filtered light. The loss of current due to the high recombination at forward bias results in a net current that is strongly bias dependent. The losses by recombination are clearly dominant near the p/i junction at high bias voltages, and they cause low FF and V_{oc} in the U-shape profile.

To increase the V_{oc} and to improve the FF, the recombination current should be lowered at high forward biases. An easy way to accomplish this is by elongating the

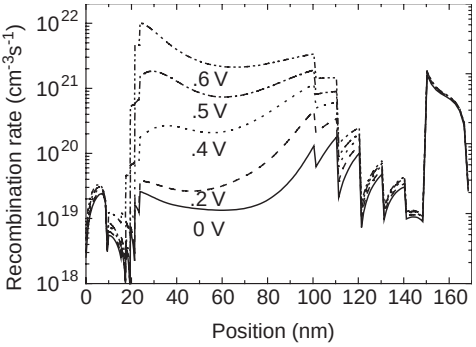

Fig. 3. Spatial recombination rate for the 'U-shape' structure under different bias conditions (filtered illuminated).

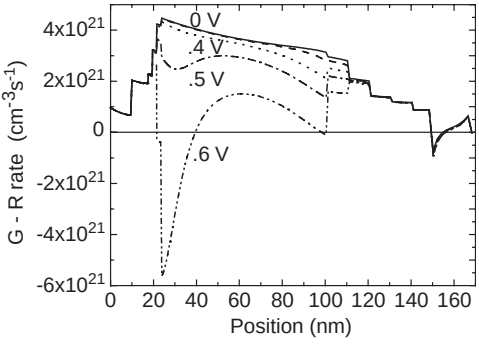

Fig. 4. Generation (G) minus spatial recombination (R) rate for the 'U-shape' structure under different bias conditions (filtered illuminated).

front and back grading and by reducing the thickness of the lowest band gap layer. Using material with a larger band gap (lower Ge concentration) reduces the density of trapped charges by reducing the defect density in the band gap. This strengthens the electric field in the bulk, and the cell thus extracts the photo-generated carriers more efficiently. Finally, the recombination losses reduce, resulting in a higher FF and V_{oc}. But this fast track approach has some drawbacks. A larger band gap material means a lower absorption coefficient and therefore a lower J_{sc}.

This indeed is the behavior observed in a V-shaped band gap profile. Fig. 2 compares the schematic band gap profile in the a-SiGe:H i-layer of a single junction having a U-shape and a V-shape profile. Table 1 displays the simulated current–voltage characteristics for the different band gap profiles. The position of the layer with the minimum band gap in the V-profile was optimized by computer simulation [9]. Under filtered light and AM 1.5 illumination, the V-shape leads to a significant improvement in V_{oc}, FF and efficiency (η), as compared to the U-shape. The deeper front grading at the p/i interface in the V-type profile decreases the charged defect state density near the p/i-interface due to the Fermi level dependence of the defect state distribution predicted by the defect pool model. Fig. 5 shows the equilibrium distribution of positively charged (D^h) and negatively charged (D^e) defect states at short circuit conditions and filtered light. The charged defect densities are

Table 1
Solar cell simulated parameters of a U-, V- and E-shape p–i–n structure under illumination conditions of AM 1.5 spectrum without and with a filter of 100 nm thick a-Si:H

		V_{oc} (V)	J_{sc} (mA/cm^2)	FF (%)	η (%)
U-shape	AM 1.5	0.72	18.3	58.9	7.72
	Filtered	0.65	6.58	59.4	2.56
V-shape	AM 1.5	0.77	17.0	62.5	8.20
	Filtered	0.71	5.75	63.7	2.61
E-shape	AM 1.5	0.74	18.0	62.4	8.33
	Filtered	0.68	6.38	63.5	2.77

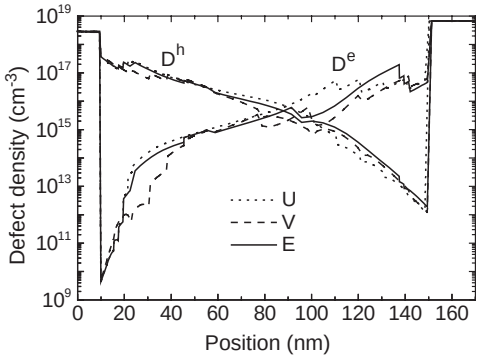

Fig. 5. Spatial distribution of positively charged (D^h) and negatively charged (D^e) defect states inside the i-layer with 'U-shape', 'V-shape' and 'E-shape' profiles at 0 V.

significantly reduced by 30% within the i-layer with a V-shape band gap profile, especially the dominant negatively charged defect (D^e) at the middle and rear part of the i-layer. The electric field improves as a result of the reduced screening introduced by space charge; it becomes more uniform inside the i-layer and decreases at the p/i and i/n junction (Fig. 6). The result is a reduction in the recombination process in the bulk of the i-layer, which in turn improves the V_{oc}. On the other hand, reduced recombination in the middle of the i-layer has an effect on FF. The larger back grading reduces the density of charged defect states in the middle and near the i/n junction. The screening effect of the electric field is reduced, improving the mobility-lifetime-electric field ($\mu\tau E$) product and thereby improving the carrier extraction decreasing the recombination in the bulk and in the rear part of the cell. Thus the FF improves due to the overall reduction of the recombination current. Together, both the front and the back grading of the V-profile lead to better performance than the U-shape. Nevertheless, the V-shape leads to a loss in the short circuit current. Fig. 7 shows the generation rate for the U- and V-shape profiles. A reduction in the optical generation is observed in the regions where the band gap has been increased. Finally,

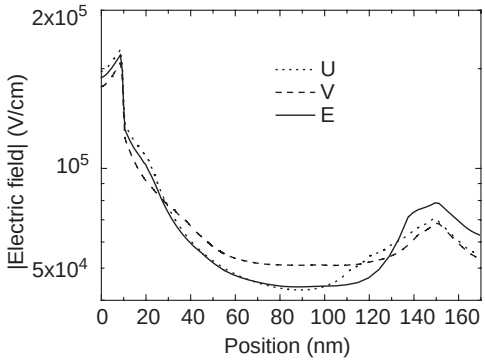

Fig. 6. Electric field within the 'U-shape', 'V-shape' and 'E-shape' profiles at 0 V.

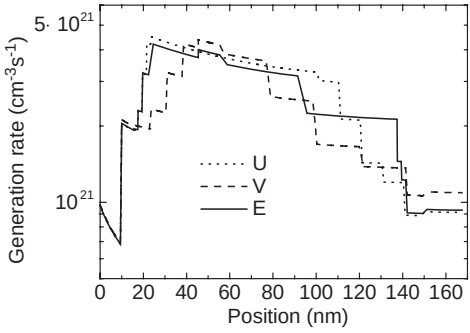

Fig. 7. Generation rate within the solar cell with 'U-shape', 'V-shape' and 'E-shape' profiles at 0 V (filtered illuminated).

the enhancement in carrier collection does not compensate the loss of photo-generated carriers.

It is necessary to have a more sophisticated band gap profile that would be capable of reducing the recombination rate but at the same time maintains the J_{sc} that a U-shape profile generates.

We have designed a band gap profile, exponential profile (E-shape profile), which reduces the recombination current, enhancing the FF and V_{oc}, and at the same time generates the same J_{sc} as the U-shape profile. With this profile, the simulations predict an improvement in efficiency of around 10%. Table 1 displays the simulated current–voltage characteristics for the three different band gap profiles. Fig. 2 shows a schematic band gap profile of the i-layer of the a-SiGe:H single junction comparing a U-shape and an E-shape profile.

In amorphous silicon alloys the main loss of carrier collection is caused by bulk recombination. To reduce the bulk recombination, the density of states in the band gap is modified by controlling the alloying of the amorphous silicon. We have gradually enlarged the front and back grading by replacing the lower band gap material in the bulk of the intrinsic i-layer by a lower alloyed, higher band gap material. The higher band gap material introduces fewer defects inside the band gap, enhancing the electronic properties.

The gradual front grading moves the position of the minimum band gap away from the p/i junction. The electron and hole quasi-Fermi levels can move further apart due to the higher band gap near the p/i interface, resulting in a higher V_{oc}. Comparing the shapes of the front grading between the E- and V-profile (Fig. 2) it is appreciated that even when both shift the minimum band gap position, the front grading of the E-shape profile generates more current, reducing the generation losses present in the V-shape profile. On the other hand the higher band gap in the front grading of the V-shape profile contributes to a higher built in potential, which we maintained in the E-shape profile.

The shape of the back grading is such that it reduces the midgap defect density in the bulk of the intrinsic layer where the electric field is weaker. Fig. 5 shows how the charged defect density, and specially the dominant D^e in the middle and rear parts of the i-layer, has been significantly reduced. Near the i/n junction the electric field is strong enough due to the high space-charge density in the highly doped n-layer. On the other side, near the p/i junction the built in potential is mainly dependent of the quality of the junction. These two ideas allow us to reduce the band gap near the i/n junction with respect to the U- and V- shape profile, while we increase it in the bulk. As we mentioned above, the material in the bulk has to host a low defect density due to the lower electric field strength in that region. This will reduce the recombination current, and improve the FF. Near the i/n junction we have decreased the band gap in order to generate the photo-current that is lost by using the higher band gap bulk material. The high electric field in this region allows us to reduce the band gap without producing important recombination losses.

Fig. 7 represents the generation profile under filtered light for the U- and E-shape band gap profile. The total generation rate is roughly the same in both profiles, with the advantage in the E-shape case of having less defect density in the bulk.

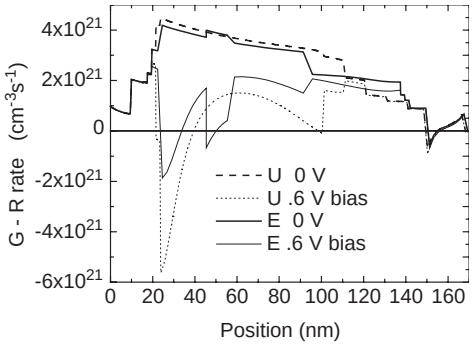

Fig. 8. Generation (G) minus spatial recombination (R) rate for the 'U-shape' and 'E-shape' structure under different bias conditions (filtered illuminated).

Fig. 8 represents the net generation (generation minus recombination) rate profiles for the U- and E- shape profile for different forward biases, under filtered light. Fig. 8 shows how the recombination current is generated as the forward bias increase. The E-shape profile presents lower recombination current than the U-shape for high forward bias, mainly in all of the bulk of the i-layer but especially near the p/i junction, resulting in an improved V_{oc}. The sharp increase in the recombination current for E-shape in the region of the lowest band gap material is due to the "pool" for the carriers created in the band gap profile for this material. At high forward bias, the band gap profile tends to be flat, reducing the electric field. The free carriers are more sensitive to the discontinuities in the band profile at this low electric field. The lowest gap material acts as a "pool" where the free carriers are temporarily trapped, increasing the recombination. This thin low band gap layer could be removed, what would increase the FF and V_{oc}, but we keep it to obtain the same total generation in the E-shape profile as in the U-profile.

In summary, we propose an exponential band gap grading of the i-layer of the a-SiGe:H single junction solar cell that generates roughly the same J_{sc} as the U-shape profile, but leads to higher FF and V_{oc}, with the result that the efficiency is improved.

Considerable effort has been made by many groups in order to obtain more efficient band gap profiles. At the same time, band gap profiles that are easier to deposit are also desirable. The group of Jülich [17] presented an interesting idea, replacing the grading by an a-Si:H buffer near the p/i junction. In contrast with this idea, our simulations predict that an appropriately designed band gap is necessary to improve the performance of the a-SiGe:H single junction even if these solar cell have a small thickness.

In the next section we show our experimental results by comparing the U-, V- and E- band gap profiles.

3.3. Experimental results

Several p–i–n single junction a-SiGe:H solar cells have been deposited with the three different band gap profiles. Table 2 shows the average solar cell characteristics

Table 2
Solar cell experimental and simulated parameters of a U-, V- and E-shape p–i–n structure under illumination conditions of AM 1.5 spectrum with a filter of 100 nm thick a-Si:H

		V_{oc} (V)	J_{sc} (mA/cm^2)	FF (%)	η (%)
U-shape	Average (experiment)	0.64 ± 0.01	6.46 ± 0.23	62 ± 2	2.57 ± 0.0
	1st simulation	0.65	6.58	59	2.56
	2nd simulation	0.64	6.55	61	2.57
V-shape	Average (experiment)	0.67 ± 0.01	5.79 ± 0.18	62 ± 1	2.43 ± 0.08
	1st simulation	0.71	5.75	64	2.61
	2nd simulation	0.68	5.88	64	2.56
E-shape	Average (experiment)	0.65 ± 0.01	6.26 ± 0.18	61 ± 2	2.54 ± 0.09
	1st simulation	0.68	6.38	64	2.77
	2nd simulation	0.66	6.72	61	2.68

for each profile. Together with the measurement appears the standard deviation of the parameter with respect to the several measured cells. The deviation does not exceed 3.5% in any of the parameters. The variation from the U- to the E-shape profile predicted by simulation is around 10%, significant to rule out statistical deviations, which could mask the results. The cells were deposited at the same time on a monitor Corning glass without TCO. The thickness of the whole cell was measured by R-T. The thickness of the different cells was the same within 10 nm. To simplify the comparison we have included the simulation values under filtered light of Table 1 as "first simulation". Where the simulations predicted a significant improvement in η in the E- and V-profiles over the U-shape profile, as has been explained in the previous section, the deposited cells show the opposite behavior. The cells with V-shape profile show a higher V_{oc} and lower J_{sc}, as predicted. This profile creates the stronger electric field in the bulk of the i-layer together with the lower defect density of states of the three profiles under study. Those properties are expected to produce a better FF in the solar cells with the V-profile. In contrast to this, the FF and η do not even reach the values that are obtained in the cells with U-shape profile. The case of the E-shape profile is more critical. Designed to improve the η and V_{oc} without losses in photo-generated current, the deposited solar cells do not present any of these improvements.

In the case of the U-shaped profile, the simulations predict lower FF and η than those obtained in the deposited solar cells.

To understand these deviations between experiment and simulation we have performed RBS measurements on samples with these three profiles and we have compared the measured band-gap profiles with the designed profiles. The H concentration was found to be uniform through the entire cell. Thus, a linear relation can appropriately be assumed between the amount of Ge in the material and the band gap. Fig. 9 shows the band gap E_G versus the position, where the zero position is the surface of the substrate.

Comparing Figs. 9 and 2 we clearly note two important differences. The first observation is that the V- and the E-shaped band gap profiles do not reach the low band gap values that are expected. The second observation is that the linear grading

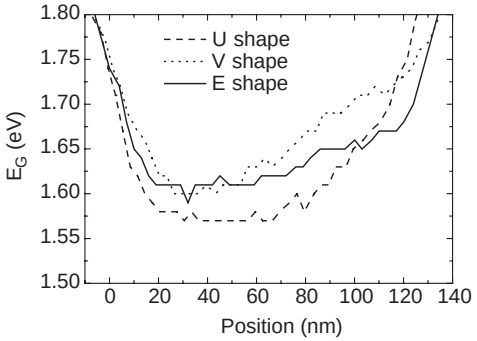

Fig. 9. Band gap profile of measured samples as calculated from the RBS Ge profiles.

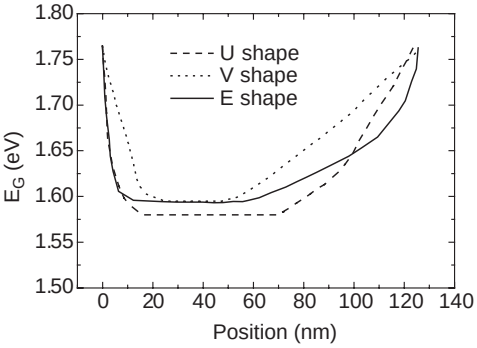

Fig. 10. Simulated band gap profiles consistent with the RBS measured profiles taking into account a delayed response of the Ge incorporated on changes in the GeH_4 flow. This is used in second simulation.

assumed from the gas flow in the U and V band gap profiles is in fact curved. This is possible as a result of a delay between the change in germane flow and the time it takes for this change in flow to produce a change in the concentration of Ge that is incorporated.

In our staircase profile, where the changes in flow follow a regularly increasing or decreasing pattern, this delay produces only a small modification to the designed profile. However, these modifications to the profile still have a significant influence on the performance of the cell, as can be appreciated in Table 2 by comparing the first and the second simulations. The uniform change in flow is the case in both the linear U- and V-shape profiles. In these two profiles the changes in the germane flow are uniform in time as well as in amount of germane to produce a linear profile in the front and back grading of the intrinsic layer. The delay modifies the expected linear profiles, however the linearity is retained. In the U-shape profile, the front and back grading are thin compared with the total intrinsic layer (the total grading is the half of the i-layer, while in the V- and E-shape the grading represents the 90% of the i-layer). Small variations in the grading will have less influence on the final cell behaviour.

Table 3
Solar cell experimental parameters of a modified E-shape p–i–n structure under illumination conditions of AM 1.5 spectrum with a filter of 100 nm thick a-Si:H

		V_{oc} (V)	J_{sc} (mA/cm^2)	FF (%)	η (%)
Modify E-Shape	Filtered	0.67 ± 0.01	6.43 ± 0.14	62 ± 0.01	2.67 ± 0.07

We have modified the band-gap profiles in the simulation and used the profiles as deduced from the Ge/Si concentrations (obtained from RBS) following the variations as caused by the delay. The modifications were done only in the thickness of step of the grading, with no intention of fitting the results but to observe if these modifications can account by them self with the mismatch between simulations and experiment. The new profiles are shown in Fig. 10. The results of these simulations are included in Table 2, as "second simulation". The small variation we have introduced in the simulation of the U-shape profile is enough to increase the η and FF, without modifying the open circuit voltage or the short circuit current. This brings the simulation closer to the experimental values and proves how a small variation of the front and back grading reduces the recombination. In the case of the V-shape profile, the variation of the band-gap profile reduces the V_{oc} and the η. The second simulation with the altered band gap grading also more closely approaches the experimental values.

The E-shape profile is more complicated to simulate by changing only the thickness of the layers. As the changes in germane flow are not uniform, the changes induced by the flow delay in the band-gap profile are larger. It may deposit in the grading a material with different characteristics than expected for the U- and V-shape profile. Introducing in the simulations the flow delay by changing the thickness of the step of the grading in the E band-gap profile, we observe how the adverse effect of this behavior accumulates.

With the knowledge of these experiments we have modified the E-shape profile in order to avoid the experimental delay and to obtain a real band gap profile closer to the goals of the original design. A p–i–n solar cell has been deposited including this correction. The characteristics of this cell are given in Table 3. It shows the intended improvements of the simulated E-shape profile: higher V_{oc}, FF and η, with low loss in J_{sc}.

4. Conclusions

We propose an exponential band gap grading of the i-layer of the narrow band gap a-SiGe:H single junction solar cells for use in the bottom solar cell in a tandem structure.

We have studied the reasons of the lower than expected efficiency of our cells by computer simulation. We found that an adequate modification of the straight grading profile is beneficial for collecting the photo-generated carriers. This is reflected by a high η, FF and V_{oc}. At the same time the new E-shape profile do not

present significant losses in J_{sc}. The trends followed by this profile are independent of the set of parameters used in the simulation, with the exception of the thickness, even when these parameters were chosen to fit the experimental data.

We showed how minor changes on the band gap profiles have a large influence in the performance of the solar cell. These small variations may be brought about by response times of flow controllers and system-dependent gas residence time. We have addressed these issues adequately with the help of RBS technique. The implementation of these small variations in computer simulations brings closer the experimental and the simulated results.

Acknowledgements

We gratefully acknowledge C.H.M. van der Werf for preparation of all the solar cell in this study. This work has been supported by the Netherlands Agency for Energy and Environment (NOVEM).

References

[1] S. Guha, J. Yang, A. Pawalikiewicz, T. Glatfelter, Appl. Phys. Lett. 54 (1989) 2330.
[2] E. Maruyama, et al., Mater. Res. Soc. Symp. Proc. 197 (1993) 821.
[3] J. Zimmer, H. Stiebig, H. Wagner, J. Appl. Phys. 84 (1998) 611.
[4] P.J. McElheny, J.K. Arch, H.S. Lin, S.J. Fonash, J. Appl. Phys. 64 (1988) 1254.
[5] H. Okamoto, H. Kida, Y. Hamakawa, Philos. Mag. B 49 (1984) 231.
[6] M.J. Powel, S.C. Deane, Phys. Rev. B 48 (1993) 10815.
[7] M.J. Powel, S.C. Deane, Phys. Rev. B 53 (1996) 10121.
[8] F.A. Rubinelli, J.D. Ouwens, R.E.I. Schropp, Proceeding of the 13th PVSEC, Nice, France, 1995, p. 195.
[9] M. Stutzmann, J. Appl. Phys. 66 (1989) 569.
[10] S. Aljishi, Z. Smith, D. Slobodin, J. Kolodzey, V. Chu, R. Schwarz, S. Wagner, Mater. Res. Soc. Symp. Proc. 70 (1986) 269.
[11] H. Stiebig, F. Siebke, R. Carius, J. Klomfab, Mater. Res. Soc. Symp. Proc. 507 (1998) 403.
[12] J. Chevalier, H. Wieder, A. Onton, C.R. Guarnieri, Solid State Commun. 24 (1977) 867.
[13] S. Aljishi, V. Chu, Z.E. Smith, J.P. Conde, D. Slobodin, J. Kolodzey, J. Non-Cryst. Solids 97&98 (1987) 1023.
[14] Z.E. Smith, S. Wagner, Phys. Rev. Lett. 59 (1987) 688.
[15] H. Stiebig, F. Siebke, W. Beyer, C. Beneking, B. Rech, H. Wagner, Solar Energy Mater. Sol. Cells 48 (1997) 351.
[16] F.A. Rubinelli, R. Jimenez Zambrano, J.K. Rath, R.E.I. Schropp, J. Appl. Phys. 91 (4) (2002) 2409.
[17] D. Lundszein, F. Finger, H. Wagner, Proceeding of the 17th PVSEC, Munich, Germany, 2001, p. 2854.